

domain V (18). Reverse transcription products were resolved by 6% denaturing polyacrylamide gel electrophoresis (PAGE), visualized, and quantitated with a Molecular Dynamics STORM PhosphorImager.

15. The A-site substrate 5' ³²P-labeled CACCPuromycin (1 μM) was reacted with CCA-Phe-Biotin (5 μM) in the presence of 50S subunits (2 μM) in buffer containing 10 mM tris HCl (pH 7.5), 100 mM NH₄Cl, 30 mM MgCl₂, and 4 mM β-mercaptoethanol at 37°C (18). Production of CACCPuromycin-Phe-Biotin was monitored as a function of time by PAGE to yield an observed rate constant of 0.03 min⁻¹ [B. E. H. Maden, R. R. Traut, R. E. Monro, *J. Mol. Biol.* **35**, 333 (1968)].
16. R. Green and H. F. Noller, *Annu. Rev. Biochem.* **66**, 679 (1997).
17. D. Moazed and H. F. Noller, *Cell* **57**, 585 (1989).
18. G. W. Muth, L. Ortoleva-Donnelly, S. A. Strobel, data not shown.
19. The DMS modification data were normalized for lane loading and extent of primer extension by dividing the peak area at each identified DMS-modified adenosine by the area of the intrinsic RT stop at nucleotides 2450 to 2447. These values were then normalized to a scale where maximum reactivity is defined as 1.0, by dividing the value for each adenosine by the value for the greatest extent of reaction (pH 8.6). The normalized modification data were fit to Eq. 2 (12):

$$I_{\text{obs}} = \frac{I_{\text{HA}}[H^+] + I_{\text{max}}}{K_a + [H^+]} \quad (2)$$

where I_{obs} is the observed extent of A2451 DMS modification at a given pH, I_{HA} is the extent of DMS reactivity for the protonated form of the nucleotide, I_{max} is the extent of reactivity for the deprotonated form of the nucleotide (defined as 1), and K_a is the equilibrium constant for protonation.
20. B. E. H. Maden and R. E. Monro, *Eur. J. Biochem.* **6**, 309 (1968).
21. S. Pestka, *Proc. Natl. Acad. Sci. U.S.A.* **69**, 624 (1972).
22. R. R. Gutell *et al.*, www.rna.icmb.utexas.edu/CSI/fts.html; R. R. Gutell, N. Larsen, C. R. Woese, *Microbiol. Rev.* **58**, 10 (1994).
23. D. Moazed and H. F. Noller, *Proc. Natl. Acad. Sci. U.S.A.* **88**, 3725 (1991).
24. P. Vannuffel, M. Di Giambattista, C. Cocito, *Nucleic Acids Res.* **22**, 4449 (1994).
25. D. Moazed and H. F. Noller, *Biochimie* **69**, 879 (1987).
26. G. Steiner, E. Kuechler, A. Barta, *EMBO J.* **7**, 3949 (1988).
27. P. Lawley and P. Brookes, *Biochem. J.* **89**, 127 (1963).
28. A. Maxam and W. Gilbert, *Proc. Natl. Acad. Sci. U.S.A.* **74**, 560 (1977).
29. T. Saito and T. Fujii, *J. Chem. Soc. Chem. Comm.* **1979**, 135 (1979).
30. The A N3 pK_a has not been reported. A related nucleoside where the N3 pK_a has been determined is 1-deazaadenosine (1dA), which has a single imino group in the six-membered pyrimidine ring (N3) with a pK_a of 4.7 [F. Seela, H. Debelak, N. Usman, A. Burgin, L. Beigelman, *Nucleic Acids Res.* **26**, 1010 (1998)]. Removal of one of the two imino groups in the pyrimidine ring markedly increases the pK_a of the remaining group. For example, the N1 pK_a of 3dA is 7.0 (ΔpK_a of +3.5 compared with A) (10), whereas the ΔpK_a between pyridine and pyrimidine is +3.9 [from J. Lister, in *The Chemistry of Heterocyclic Compounds*, D. J. Brown, Ed. (Wiley, New York, 1971), pp. 448–453]. Assuming that the N3 of 1dA has a similar ΔpK_a because of removal of the N1 imino group, the unperturbed pK_a of A N3 would be about 4.7 – 3.7 = 1.0.
31. S. E. Kearsey and I. W. Craig, *Nature* **290**, 607 (1981).
32. A2451 was mutated to G, C, or U in the plasmid pLK35, which contains the rrnB operon under control of the bacteriophage λ P₁ promoter [S. Douthwaite, T. Powers, J. Y. Lee, H. F. Noller, *J. Mol. Biol.* **209**, 655 (1989)]. The mutant plasmids were transformed into pop2136 cells, an *E. coli* strain that expresses an integrated temperature sensitive form of λ repressor. In these cells, rrnB expression is induced at high temperature (42°C). Cells containing the wild type and three mutant plasmids were grown on 2xYT media containing 60 μg/ml of ampicillin at 30°C or 42°C.
33. J. Kraut, *Annu. Rev. Biochem.* **46**, 331 (1977).

34. T. Steitz and R. Shulman, *Annu. Rev. Biophys. Bioeng.* **11**, 419 (1982).
35. We thank A. Dahlberg for plasmid pLK35 and *E. coli* strain pop2136, B. Freeborn and A. Kosek for technical assistance, T. A. Steitz and P. B. Moore for information about the 50S structure before publication, D. M. Crothers and S. P. Ryder for helpful discussion,

and L. Weinstein, J. A. Doudna, A. A. Szwczak, and A. K. Oyelere for critical comments on this manuscript. This work was supported by a Basil O'Connor Award from the March of Dimes and NIH grant GM54839. G.W.M. is the recipient of an Anderson postdoctoral fellowship.

29 June 2000; accepted 24 July 2000

Inhibition of Adipogenesis by Wnt Signaling

Sarah E. Ross,¹ Nahid Hemati,¹ Kenneth A. Longo,¹ Christina N. Bennett,¹ Peter C. Lucas,² Robin L. Erickson,¹ Ormond A. MacDougald^{1*}

Wnts are secreted signaling proteins that regulate developmental processes. Here we show that Wnt signaling, likely mediated by Wnt-10b, is a molecular switch that governs adipogenesis. Wnt signaling maintains preadipocytes in an undifferentiated state through inhibition of the adipogenic transcription factors CCAAT/enhancer binding protein α (C/EBPα) and peroxisome proliferator-activated receptor γ (PPARγ). When Wnt signaling in preadipocytes is prevented by overexpression of Axin or dominant-negative TCF4, these cells differentiate into adipocytes. Disruption of Wnt signaling also causes transdifferentiation of myoblasts into adipocytes *in vitro*, highlighting the importance of this pathway not only in adipocyte differentiation but also in mesodermal cell fate determination.

Adipocytes arise from mesodermal stem cells, which have the capacity to differentiate into a variety of other cell types, including myocytes (1). Once committed to the adipocyte lineage, preadipocytes can remain quiescent, multiply, or undergo differentiation and become adipocytes. 3T3-L1 and 3T3-F442A cells are established mouse preadipocyte models. Both cell lines can be induced to differentiate in cell culture, but 3T3-F442A cells are thought to be arrested at a later point in development (2). Studies of these cellular models have revealed some of the molecular events that orchestrate adipogenesis, including the role of C/EBPs and PPARγ in mediating the expression of adipocyte-specific genes (3, 4).

Wnts are a family of paracrine and autocrine factors that regulate cell growth and cell fate (5). Signaling is initiated when Wnt ligands bind to transmembrane receptors of the Frizzled family. In the canonical Wnt signaling pathway, Frizzleds signal through Dishevelled to inhibit the kinase activity of a complex containing glycogen synthase kinase 3 (GSK3), Axin, β-catenin, and other proteins. This complex targets β-catenin for rapid degradation through phosphorylation. Thus, once hypophosphorylated due to Wnt signaling, β-catenin is stabilized and translo-

cates to the nucleus where it binds the TCF/LEF family of transcription factors to regulate the expression of Wnt target genes (5–7).

To examine the role of Wnt signaling in adipogenesis, we tested whether Wnt expression in 3T3-L1 preadipocytes affected their ability to differentiate. We used Wnt-1 in these experiments because related cell lines, such as NIH-3T3 cells, respond to this ligand (8). In addition, we used two approaches to activate Wnt signaling downstream of the receptor: (i) treatment of cells with lithium, which inhibits GSK3 activity (9), and (ii) expression of a β-catenin mutant (β-catS33Y), which increases β-catenin stability (10). The 3T3-L1 preadipocytes were infected with a retrovirus vector alone (pLXSN) or retroviruses carrying either the genes for Wnt-1 (11) or β-catS33Y. After selection, cells were induced to differentiate in 10% fetal calf serum with methylisobutylxanthine, dexamethasone, and insulin (MDI). Control cells differentiated into adipocytes, as assessed by Oil Red-O staining and by immunoblot detection of the adipocyte fatty acid binding protein, 422/aP2 (12), whereas cells expressing Wnt-1 failed to differentiate (Fig. 1A). Neither lipid droplets nor 422/aP2 were detected in Wnt-1-expressing cells (12). Inhibition of differentiation was also observed when Wnt signaling was activated by lithium or β-catS33Y (Fig. 1A). Thus, Wnt signaling appears to inhibit adipogenesis *in vitro*.

Next, we used a model of adipocyte differentiation in which 3T3-F442A preadipocytes are injected subcutaneously into athymic mice (13, 14). Over several weeks, these

¹Department of Physiology, ²Department of Pathology, University of Michigan Medical School, Ann Arbor, MI 48109–0622, USA.

*To whom correspondence should be addressed. E-mail: macdouga@umich.edu

REPORTS

cells differentiate into adipocytes, forming a discrete fat pad. Seven weeks after implantation, we found that control pLXSN-infected cells differentiated into unilocular and multilocular adipocytes, whereas cells expressing Wnt-1 formed pads composed entirely of undifferentiated, fibroblast-like cells (Fig. 1B). These results indicate that Wnt signaling can repress adipocyte differentiation in a more physiological model.

To gain mechanistic insight into the inhibition of adipogenesis, we examined the effect of Wnt-1 on expression of regulatory genes in the adipogenic program. After induction of differentiation, control and Wnt-1-expressing cells showed a similar pattern of C/EBP β and C/EBP δ expression (12). Likewise, Wnt-1 had no effect on the expression of c-Myc (15) and CHOP (12). In contrast, C/EBP α and PPAR γ , two proteins normally required for adipocyte differentiation (16, 17), were undetectable in Wnt-1-expressing cells at either the protein level (Fig. 1C) or the RNA level (12).

To test whether expression of C/EBP α and PPAR γ could rescue differentiation of Wnt-1-expressing cells, we infected 3T3-L1 cells with retroviruses carrying the genes for C/EBP α or PPAR γ (18). After selection, cells were induced to differentiate with MDI. Three weeks later, control cells (Fig. 2A) and those expressing C/EBP α alone (Fig. 2B) differentiated into adipocytes that stained vividly with Oil Red-O. Cells expressing PPAR γ also differentiated into adipocytes, although these cells contained smaller fat droplets that stained less intensely (Fig. 2C). Cells expressing Wnt-1 alone remained fibroblastic (Fig. 2D). However, when C/EBP α or PPAR γ was coexpressed, ~25% of the cells differentiated into adipocytes (Fig. 2, E and F). Expression of the adipocyte marker, 422/aP2, correlated with the degree of differentiation (12). These results suggest that Wnt-1 represses differentiation by inhibiting the expression of the C/EBP α and PPAR γ transcription factors.

To investigate the role of endogenous Wnt signaling in preadipocytes, we inhibited the Wnt pathway in 3T3-L1 cells by expression of dominant-negative TCF4 (dnTCF4) (10), which cannot be activated by β -catenin (19) but does bind to TCF/LEF consensus binding sites. Cells were infected with a retrovirus carrying the dnTCF4 gene and were maintained in 10% calf serum. Whereas control cells failed to differentiate under these conditions, ~35% of cells expressing dnTCF4 underwent adipogenesis (Fig. 3A), accompanied by expression of C/EBP α , PPAR γ , and 422/aP2 (Fig. 3B). Ectopic expression of dnTCF4 also induced adipogenesis of C3H10T1/2 cells and NIH-3T3 fibroblasts (12), suggesting that many cell types with adipogenic potential are restrained

from this fate by Wnt signaling.

We also tested the effects of a different inhibitor of the Wnt signaling pathway, Axin, which acts by facilitating the phosphorylation (and therefore degradation) of β -catenin (6). Ectopic expression of Axin (20) in 3T3-L1 preadipocytes promoted their differentiation into adipocytes in the absence of inducing agents (Fig. 3C). Consistent with the hypoth-

esis that endogenous Wnt signaling inhibits adipogenesis, free cytosolic β -catenin was found to decrease dramatically over the course of adipocyte differentiation (Fig. 3D).

Unlike 3T3-F442A cells, 3T3-L1 preadipocytes do not undergo adipogenesis when injected into athymic mice (14). To test whether Wnt signaling inhibits differentiation of 3T3-L1 cells in this in vivo model, we

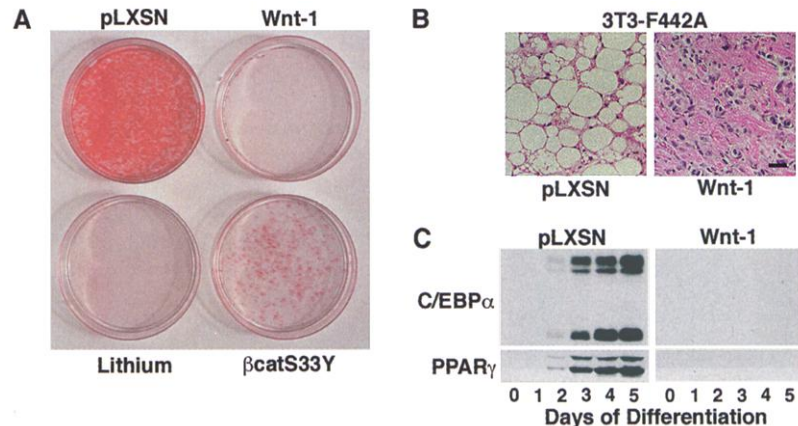
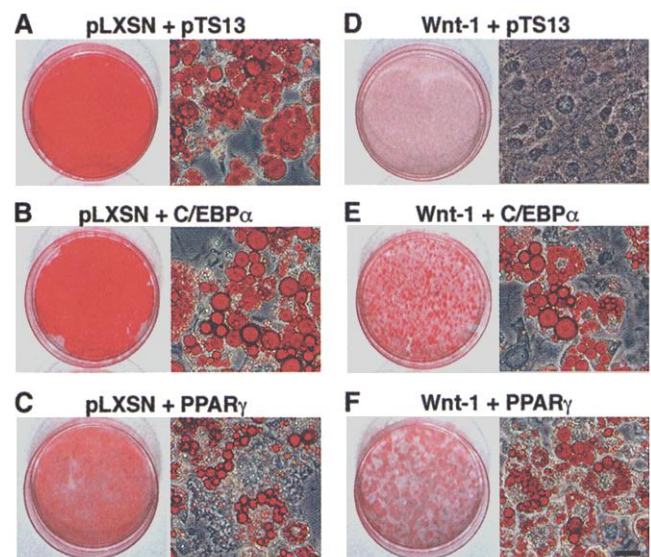


Fig. 1. (A) Wnt signaling blocks adipogenesis in vitro. 3T3-L1 preadipocytes were infected with a retrovirus vector alone (pLXSN) or retroviruses carrying the genes for Wnt-1 (11) or β -catS33Y (10) using standard methods (25). Two days post-confluence, cells were induced to differentiate with MDI (26). A second pLXSN-infected plate was induced to differentiate in the continuous presence of 25 mM LiCl (Lithium). Treatment of cells with 25 mM NaCl does not inhibit differentiation (27). Three weeks later, cells were stained with Oil Red-O (27) to visualize the degree of lipid accumulation. In vitro data in this and subsequent figures are representative of at least three independent experiments. (B) Wnt-1 blocks adipogenesis in vivo. 3T3-F442A preadipocytes were infected with a retrovirus vector alone (pLXSN) or a retrovirus carrying the Wnt-1 gene. After selection, cells were treated with trypsin and were injected subcutaneously into athymic mice (73, 74). Seven weeks later, the resulting tissue was dissected, fixed in formalin, and embedded in paraffin wax. Sections were stained with hematoxylin and eosin. Bar, 16 μ m. In vivo data here and in Fig. 3E are representative of at least two or three animals. (C) Wnt signaling blocks induction of C/EBP α and PPAR γ . 3T3-L1 preadipocytes were infected with a retrovirus vector alone (pLXSN) or a retrovirus carrying the Wnt-1 gene. Two days post-confluence, cells were induced to differentiate with MDI and were lysed at the times indicated for immunoblot analyses of C/EBP α (26) and PPAR γ (Santa Cruz Biotechnology, Inc., Santa Cruz, CA). There are three forms of C/EBP α (28): p42C/EBP α (top), p40C/EBP α (middle), and p30C/EBP α (bottom), and two forms of PPAR γ (29): γ 2 (top) and γ 1 (bottom).

Fig. 2. C/EBP α and PPAR γ partially rescue adipocyte differentiation of Wnt-1-expressing cells. Control (pLXSN) or Wnt-1-expressing cells were reinfected with a retrovirus vector alone (pTS13) (A and D) or retroviruses carrying the genes for C/EBP α (B and E) or PPAR γ (C and F) (18) and were co-selected with G418 and hygromycin. Two days post-confluence, cells were induced to differentiate with MDI. PPAR γ -infected cells were induced with MDI and 5 μ M troglitazone. Three weeks later, cells were stained with Oil Red-O. Plates of cells (100 mm) and micrographs are shown. Bar, 20 μ m.



REPORTS

examined the effect of ectopic dnTCF4 expression. Seven weeks after implantation, control cells remained undifferentiated,

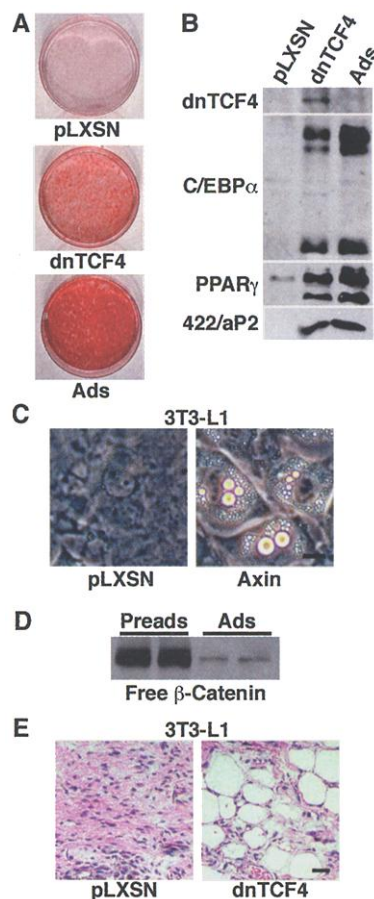


Fig. 3. (A) DnTCF4 causes spontaneous adipogenesis of 3T3-L1 cells in vitro. Preadipocytes were infected with a retrovirus vector alone (pLXSN) or a retrovirus carrying the dnTCF4 gene and were maintained in 10% calf serum. Two weeks post-confluence, these cells and (for comparison) 3T3-L1 adipocytes (Ads) were stained with Oil Red-O. (B) DnTCF4-induced adipogenesis is accompanied by expression of C/EBP α , PPAR γ , and 422/aP2, as assessed by immunoblot analyses. Flag-tagged dnTCF4 was analyzed with antibody to Flag (Sigma). (C) Phase contrast micrograph showing Axin-induced adipogenesis of 3T3-L1 cells. The 3T3-L1 preadipocytes were infected with a retrovirus vector alone (pLXSN) or a retrovirus carrying the gene for Axin (20) and were maintained in the absence of differentiation media. Many Axin-expressing cells differentiated into adipocytes within a few days, whereas control cells did not. Bar, 20 μ m. (D) Free cytosolic β -catenin decreases during adipocyte differentiation. Cytosolic fractions from confluent 3T3-L1 preadipocytes (Preads) and fully differentiated 3T3-L1 adipocytes (Ads) were analyzed by immunoblot for β -catenin (11). (E) DnTCF4 causes spontaneous adipogenesis of 3T3-L1 cells in vivo. Preadipocytes were infected with a retrovirus vector alone (pLXSN) or a retrovirus carrying the dnTCF4 gene and were injected subcutaneously into athymic mice (13, 14). Seven weeks later, the resulting tissue was dissected and fixed. Sections were stained with hematoxylin and eosin. Bar, 16 μ m.

whereas ~25% of the implanted dnTCF4-expressing cells had differentiated into adipocytes (Fig. 3E). Thus, the inability of 3T3-L1 cells to differentiate in vivo appears to be due to endogenous Wnt signaling.

Other laboratories have shown that Wnt signaling is a positive regulator of myogenesis (21, 22). Because adipocytes and myocytes originate from the same precursor cell, we speculated that Wnt signaling is important for the cell fate decision leading to muscle or fat. To test this idea, we expressed dnTCF4 in C2C12 myoblasts and found that these cells differentiated into adipocytes, as assessed by Oil Red-O staining (Fig. 4A) and expression of an adipocyte marker, 422/aP2 (Fig. 4B). Similar results were observed with a second myoblast model, G8 cells. The transdifferentiation of these myoblasts suggests that active Wnt signaling is required for continued commitment to the myocyte lineage.

The finding that inhibition of Wnt signaling in preadipocytes and myoblasts induces adipogenesis suggests that these mesodermal cells resist entry into the adipogenic program by secreting a member of the Wnt family. We therefore determined which Wnts were ex-

pressed in 3T3-L1 cells. Using a combination of reverse transcriptase-polymerase chain reaction (RT-PCR) with pan-specific Wnt primers (23) and ribonuclease protection analyses, we identified Wnt-5a and Wnt-10b. Of these, only Wnt-10b was able to stabilize free cytosolic β -catenin (Fig. 4C) and block adipogenesis when ectopically expressed (Fig. 4D). Analysis of Wnt-10b mRNA over the course of 3T3-L1 adipocyte differentiation revealed that its expression was highest in growing and confluent cells, but decreased upon MDI treatment (Fig. 4E), which is consistent with the idea that a decrease in Wnt-10b is required for adipogenesis to occur. Wnt-10b may act through TCF4, which is constitutively expressed throughout adipocyte differentiation (Fig. 4E). In accordance with our suggestion that Wnt signaling underlies the different adipogenic tendencies of 3T3-L1 and 3T3-F442A cells, Wnt-10b is expressed at much higher levels in 3T3-L1 preadipocytes than 3T3-F442A cells (Fig. 4F). Collectively, these data suggest that Wnt-10b is an endogenous regulator of adipogenesis.

In summary, we report that Wnt signaling functions as an adipogenic switch.

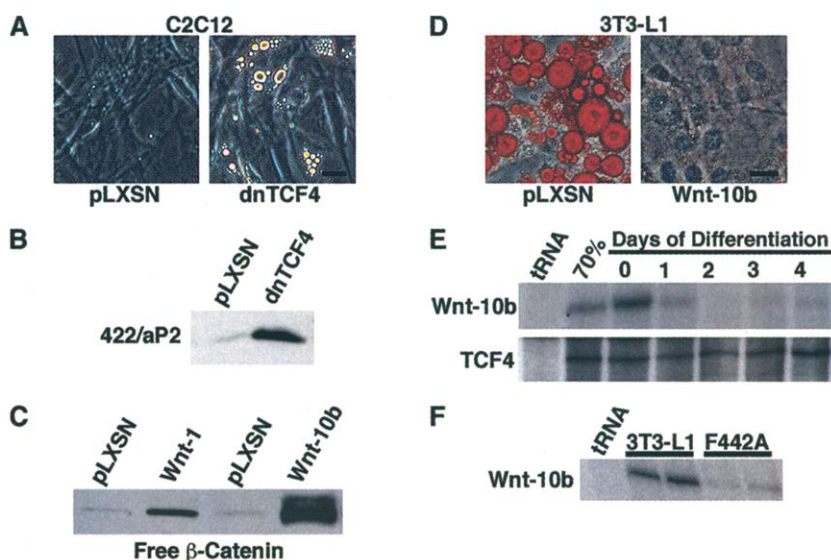


Fig. 4. (A) DnTCF4 causes transdifferentiation of C2C12 myoblasts into adipocytes. C2C12 myoblasts were infected with a retrovirus vector alone (pLXSN) or a retrovirus carrying the dnTCF4 gene and were maintained in 10% fetal calf serum. Within 2 weeks, some dnTCF4-infected cells acquired lipid. Bar, 20 μ m. (B) DnTCF4-mediated transdifferentiation is accompanied by expression of the adipocyte marker 422/aP2, as assessed by immunoblot analysis. Trace signal in control C2C12 myoblasts (pLXSN) is likely due to cross reactivity of the 422/aP2 antibody with a muscle isoform of the fatty acid binding protein. (C) Wnt-1 and Wnt-10b stabilize free cytosolic β -catenin in 3T3-L1 cells. Preadipocytes were infected with a retrovirus vector alone (pLXSN) or a retrovirus carrying the genes for Wnt-1 or Wnt-10b (30). Cytosolic fractions were analyzed for β -catenin by immunoblot (11). (D) Wnt-10b blocks adipogenesis of 3T3-L1 preadipocytes in vitro. Two days post-confluence, control (pLXSN) and Wnt-10b-infected cells were induced to differentiate with MDI (26). Two weeks later, cells were stained with Oil Red-O. Bar, 20 μ m. Representative micrographs are shown. (E) Wnt-10b is repressed during differentiation of 3T3-L1 preadipocytes. RNA was isolated from cells that were 70% confluent (70%), 2 days post-confluent (Day 0), and cells that had been induced with MDI for the number of days indicated. Ribonuclease protection analysis (31) with probes for mouse Wnt-10b [amplified by PCR (24)] and TCF4 (32). Yeast tRNA served as the control for background protection. (F) Wnt-10b is expressed at higher levels in 3T3-L1 cells than in 3T3-F442A cells, as assessed by ribonuclease protection analysis of RNA from confluent cells.

When it is on, adipogenesis is repressed; when it is off, adipogenesis is initiated. The crucial role of Wnt signaling in the adipogenic program is emphasized by the finding that in its absence, myoblasts are reprogrammed to the adipocyte lineage and undergo spontaneous differentiation.

References and Notes

1. P. Cornelius, O. A. MacDougald, M. D. Lane, *Annu. Rev. Nutr.* **14**, 99 (1994).
2. O. A. MacDougald and M. D. Lane, *Annu. Rev. Biochem.* **64**, 345 (1995).
3. G. J. Darlington, S. E. Ross, O. A. MacDougald, *J. Biol. Chem.* **273**, 30057 (1998).
4. B. M. Spiegelman, *Diabetes* **47**, 507 (1998).
5. K. M. Cadigan and R. Nusse, *Genes Dev.* **11**, 3286 (1997).
6. A. Kikuchi, *Cytokine Growth Factor Rev.* **10**, 255 (1999).
7. J. R. Miller, A. M. Hocking, J. D. Brown, R. T. Moon, *Oncogene* **18**, 7860 (1999).
8. A. Bafico, A. Gazit, S. S. Wu-Morgan, A. Yaniv, S. A. Aaronson, *Oncogene* **16**, 2819 (1998).
9. P. S. Klein and D. A. Melton, *Proc. Natl. Acad. Sci. U.S.A.* **93**, 8455 (1996).
10. F. T. Kolligs, G. Hu, C. V. Dang, E. R. Fearon, *Mol. Cell. Biol.* **19**, 5696 (1999).

11. C. S. Young, M. Kitamura, S. Hardy, J. Kitajewski, *Mol. Cell. Biol.* **18**, 2474 (1998).
12. S. E. Ross, N. Hemati, O. A. MacDougald, data not shown.
13. H. Green and O. Kehinde, *J. Cell. Physiol.* **101**, 169 (1979).
14. S. Mandrup, T. M. Loftus, O. A. MacDougald, F. P. Kuhajda, M. D. Lane, *Proc. Natl. Acad. Sci. U.S.A.* **94**, 4300 (1997).
15. Although Wnt-1 is a mitogen in many cell types and caused elevated cyclin D1 in 3T3-L1 preadipocytes, its expression did not alter the number of cells at confluence or during MDI-induced clonal expansion, nor did it cause an elevation in c-Myc protein.
16. N.-d. Wang et al., *Science* **269**, 1108 (1995).
17. B. D. Lowell, *Cell* **99**, 239 (1999).
18. D. Shao and M. A. Lazar, *J. Biol. Chem.* **272**, 21473 (1997).
19. V. Korinek et al., *Science* **275**, 1784 (1997).
20. M. A. Julius et al., in preparation.
21. S. Hoppler, J. D. Brown, R. T. Moon, *Genes Dev.* **10**, 2805 (1996).
22. G. Cossu and U. Borello, *EMBO J.* **18**, 6867 (1999).
23. Primers and PCR reactions were as described in (24). A second PCR reaction was performed with a sense primer that is one nucleotide shorter at the 3' end. PCR products were analyzed on agarose gels, cloned into pCR II (Invitrogen, Carlsbad, CA) and sequenced.
24. J. L. Christian, B. J. Gavin, A. P. McMahon, R. T. Moon, *Dev. Biol.* **143**, 230 (1991).

25. A. D. Miller and G. J. Rosman, *Biotechniques* **7**, 980 (1989).
26. N. Hemati, S. E. Ross, R. L. Erickson, G. E. Groblewski, O. A. MacDougald, *J. Biol. Chem.* **272**, 25913 (1997).
27. S. E. Ross, R. L. Erickson, N. Hemati, O. A. MacDougald, *Mol. Cell. Biol.* **19**, 8433 (1999).
28. F.-T. Lin, O. A. MacDougald, A. M. Diehl, M. D. Lane, *Proc. Natl. Acad. Sci. U.S.A.* **90**, 9606 (1993).
29. P. Tontonoz, E. Hu, B. M. Spiegelman, *Cell* **79**, 1147 (1994).
30. D. J. Van Den Berg, A. K. Sharma, E. Bruno, R. Hoffman, *Blood* **92**, 3189 (1998).
31. O. A. MacDougald, C.-S. Hwang, H. Fan, M. D. Lane, *Proc. Natl. Acad. Sci. U.S.A.* **92**, 9034 (1995).
32. E. A. Cho and G. R. Dressler, *Mech. Dev.* **77**, 9 (1998).
33. We thank M. A. Lazar, J. Kitajewski, E. Fearon, D. J. Van Den Berg, and G. Dressler for plasmids; D. A. Bernlohr for antibody to 422/aP2; and K. Cadigan, C. Carter-Su, K. L. Guan, E. Fearon, and J. Williams for critical review of the manuscript. Supported in part by grants from the NIH (RO1-DK51563 to O.A.M.), the Natural Sciences and Engineering Research Council of Canada (S.E.R. and R.L.E.), the University of Michigan Endocrinology and Metabolism Fellowship Training Grant T32-DK07245 (K.A.L.), and the Michigan Diabetes Research and Training Center (NIH 5P60 DK20572).

9 June 2000; accepted 26 June 2000

Calcium Sensitivity of Glutamate Release in a Calyx-Type Terminal

Johann H. Bollmann,^{1*} Bert Sakmann,¹ J. Gerard G. Borst^{1,2}

Synaptic efficacy critically depends on the presynaptic intracellular calcium concentration ($[Ca^{2+}]_i$). We measured the calcium sensitivity of glutamate release in a rat auditory brainstem synapse by laser photolysis of caged calcium. A rise in $[Ca^{2+}]_i$ to 1 micromolar readily evoked release. An increase to >30 micromolar depleted the releasable vesicle pool in <0.5 millisecond. A comparison with action potential-evoked release suggested that a brief increase of $[Ca^{2+}]_i$ to ~10 micromolar would be sufficient to reproduce the physiological release pattern. Thus, the calcium sensitivity of release at this synapse is high, and the distinction between phasic and delayed release is less pronounced than previously thought.

In response to an action potential, the presynaptic release probability is strongly increased for a few milliseconds. This phasic release is thought to be triggered by a brief, localized increase in $[Ca^{2+}]_i$ in the vicinity of open, presynaptic Ca^{2+} channels. The Ca^{2+} sensitivity of phasic release in mammalian central synapses is not yet known. On the basis of results obtained in other synapses, it has been assumed that a low-affinity Ca^{2+} sensor, which is activated by local increases of $[Ca^{2+}]_i$ to >100 μ M, triggers phasic release in mammalian cen-

tral synapses (1-4). In contrast, the more prolonged, delayed release period that, at most synapses, follows the phasic release may be controlled by a separate Ca^{2+} sensor with a much higher affinity for Ca^{2+} (5).

We measured the Ca^{2+} sensitivity of glutamate release at a giant synapse in the auditory brainstem, the axosomatic synapse formed by the calyx of Held with a principal cell in the medial nucleus of the trapezoid body. Using laser photolysis of caged Ca^{2+} , we compared in the same terminals release evoked by a sustained, spatially uniform rise in presynaptic $[Ca^{2+}]_i$ (6) with release triggered by action potentials, during which changes in $[Ca^{2+}]_i$ are transient and highly localized (3). In 9-day-old rats, this synapse shows prominent synaptic depression during high-frequency signaling, which is most likely caused by rapid depletion of the releasable pool of vesicles (6-8). In

order to relate the flash-evoked excitatory postsynaptic currents (EPSCs) to the size of the releasable pool in the same terminal, we first estimated the releasable pool size in the intact terminal. Simultaneous pre- and postsynaptic recordings were made from the calyx and a principal cell (9). With the presynaptic recording still in the cell-attached configuration, a train of action potentials was evoked by an extracellular electrode (Fig. 1A). A measure of release was obtained from the amplitudes of the glutamatergic EPSCs simultaneously recorded in the principal cell. During the train, the size of the EPSCs rapidly depressed, reaching a steady state within 100 ms. The cumulative amplitude of the EPSCs evoked by a train of afferent stimuli (200 ms, 200 Hz) was taken as a measure of the size of the releasable pool (7). This estimate was corrected for the steady-state component in the EPSCs (Fig. 1B). The cumulative EPSC was -9.7 ± 0.7 nA ($n = 43$, mean \pm SEM) at a holding potential of -30 mV. The quantal EPSC amplitude was -32 ± 2 pA ($n = 10$ cells) at -80 mV. Assuming that the release of one vesicle gives an EPSC amplitude of -12 pA at -30 mV, this gave a releasable pool size of 810 ± 60 vesicles (6, 7). The amplitude of the first EPSC was $21 \pm 2\%$ ($n = 43$) of the amplitude of the cumulative EPSC. Taking the decay of the quantal EPSC into account, this means that about one-quarter of the releasable vesicle pool is released by a single action potential. In the presence of cyclothiazide, the 20 to 80% rise time of a single action potential-evoked EPSC was 424 ± 11 μ s ($n = 43$). Its time course was not different at holding potentials of -80 and -30 mV (paired t test, $P > 0.05$; $n = 7$).

After establishing the whole-cell configuration, the terminal was loaded via the patch

¹Max-Planck-Institute for Medical Research, Department of Cell Physiology, Jahnstrasse 29, D-69120 Heidelberg, Germany. ²Swammerdam Institute for Life Sciences, University of Amsterdam, Kruislaan 320, 1098 SM Amsterdam, the Netherlands.

*To whom correspondence should be addressed. E-mail: jbollman@mpimf-heidelberg.mpg.de